Synthesis, Crystal Structure and Solution Fluxionality of Heterometallic Hydride Clusters $[WRu_3L(CO)_{11}(\mu\text{-}H)_2(AuPPh_3)]$ ($L = C_5H_5$ or C_5Me_5)†

Chi-Chung Chen,[a] Yun Chi,*[,a] Shie-Ming Peng*[,b] and Gene-Hsiang Lee[b]
[a] *Department of Chemistry, National Tsing Hua University, Hsinchu 30043, Taiwan, Republic of China*
[b] *Department of Chemistry, National Taiwan University, Taipei 10764, Taiwan, Republic of China*

Two heterometallic compounds $[WRu_3L(CO)_{11}(\mu\text{-}H)_2(AuPPh_3)]$ ($L = C_5H_5$ **1** or C_5Me_5 **2**) were prepared by hydrogenation of $[WRu_3L(CO)_{12}(AuPPh_3)]$ in refluxing tetrahydrofuran solution. The C_5H_5 derivative possesses a tetrahedral Ru_3W core in which the $AuPPh_3$ unit bridges a Ru–Ru edge, one hydride caps a nearby WRu_2 face and the second spans a Ru–Ru edge, whereas the corresponding C_5Me_5 derivative adopts a related but distinct molecular geometry in the solid state, in which both hydride ligands span the equivalent Ru–W edges and the $AuPPh_3$ unit is linked to the Ru atoms supporting the hydrides. The dynamic processes in solution were established for these two derivatives. Crystal data for **1**: monoclinic, space group $P2_1/c$; $a = 9.031(2)$, $b = 25.086(4)$, $c = 16.238(3)$ Å, $\beta = 95.75(2)°$, $Z = 4$; final $R = 0.036$, $R' = 0.032$ for 4391 reflections with $I > 2\sigma(I)$. Crystal data for **2**: space group $Pna2_1$; $a = 20.389(3)$, $b = 16.226(3)$, $c = 26.074(4)$ Å, $Z = 8$; final $R = 0.040$, $R' = 0.036$ for 4556 reflections with $I > 2\sigma(I)$.

The chemistry of mixed-metal clusters of transition-metals has been the subject of considerable research activity.[1] A major reason for this is that the various metals present in mixed-metal clusters may show reactivity patterns or structures very different from those of the homometallic analogues. With the objective to examine the crystal structure and bonding of the heterometal polyhydride clusters, we have previously synthesised and fully characterized a series of tetrahedral clusters $[WM_3L(CO)_{11}(\mu\text{-}H)_3]$ ($M = Os$, $L = C_5H_5$ **3** or C_5Me_5 **4**; $M = Ru$, $L = C_5H_5$ **5** or C_5Me_5 **6**) by hydrogenation of cluster compounds $[WM_3L(CO)_{12}(\mu\text{-}H)]$.[2] In the solid state compounds **3**–**6** adopt a tetrahedral M_3W core in which the hydride ligands bridge three edges of a M_2W triangle (Scheme 1). However, the C_5H_5 derivatives **3** and **5** exhibit rapid

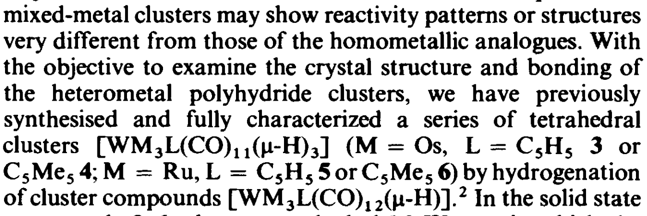

Scheme 1

tautomerization in solution, generating a minor isomer **b** in which the hydrides take up one W–M edge and two M–M edges are arranged in a zigzag arrangement. This zigzag arrangement of hydride was also observed in the related clusters $[MoM_3(\eta\text{-}C_5H_5)(CO)_{11}(\mu\text{-}H)_3]$ ($M = Os$ and Ru) and further confirmed by single-crystal X-ray diffraction.[3] The intramolecular tautomerization through hydride migration is related to that reported for the anionic cluster complex $[Ru_4(CO)_{12}(\mu\text{-}H)_3]^-$.[4]

As part of our continuing investigation on this subject, we prepared two additional Ru_3W clusters $[WRu_3L(CO)_{11}(\mu\text{-}H)_2(AuPPh_3)]$ ($L = C_5H_5$ **1** or C_5Me_5 **2**), with an isolobal $AuPPh_3$ fragment formally replacing a bridging hydride. The introduction of the $AuPPh_3$ fragment compels the hydride to adopt a triply bridging mode for the C_5H_5 derivative **1** and induces formation of two interconverting isomers, upon dissolution of the C_5Me_5 derivative **2**. In this paper we report the preparation and characterization of compounds **1** and **2** and present variable-temperature NMR studies on hydride migration and intramolecular tautomerization.

Experimental

General.—Infrared spectra were recorded on a Bomen M-100 FT-IR spectrometer. Proton, ^{13}C and ^{31}P NMR spectra were recorded on a Bruker AM-400 (400.13 MHz) or a AMX-300 (300.6 MHz) instrument. Mass spectra were obtained on a JEOL-HX110 spectrometer operating in fast atom bombardment (FAB) mode. All reactions were performed under a nitrogen atmosphere using deoxygenated solvents dried with an appropriate reagent. The progress of reactions was monitored by analytical thin-layer chromatography (5735 Kieselgel 60 F_{254}, E. Merck) and the products were separated on commercially available preparative thin-layer chromatographic plates (Kieselgel 60 F_{254}, E. Merck). The complexes $[WRu_3L(CO)_{12}(AuPPh_3)]$ ($L = C_5H_5$ or C_5Me_5) were prepared from the reaction of cluster anions $[WRu_3L(CO)_{12}]^-$, prepared from the reaction of $[Ru_3(CO)_{12}]$ and salts $[N(PPh_3)_2][WL(CO)_3]$,[5] with $[Au(PPh_3)Cl]$ in the presence of $TlPF_6$.[6] Elemental analyses were performed at the NSC Regional Instrument Center at National Cheng Kung University, Tainan, Taiwan.

Synthesis of Complexes **1** *and* **2**.—A tetrahydrofuran (thf) solution (30 cm^3) of $[WRu_3(\eta\text{-}C_5H_5)(CO)_{12}(AuPPh_3)]$ (100 mg, 0.074 mmol) was refluxed under 1 atm of hydrogen for 30 min, during which it changed from green to red-brown. After cooling the solution to room temperature, the solvent was evaporated *in vacuo* and the residue was separated by thin-layer chromatography [dichloromethane–hexane (1:1)], giving 94 mg of red-brown $[WRu_3(\eta\text{-}C_5H_5)(CO)_{11}(\mu\text{-}H)_2(AuPPh_3)]$ **1** (0.071 mmol, 96%). The respective C_5Me_5 derivative **2** was prepared analogously in 88% yield. Crystals of **1** and **2** suitable for X-ray analysis were recrystallized from a layered solution of dichloromethane–methanol at room temperature.

† *Supplementary data available:* see Instructions for Authors, *J. Chem. Soc., Dalton Trans.*, 1993, Issue 1, pp. xxiii–xxviii.
Non-SI unit employed: atm = 101 325 Pa.

Table 1 Experimental data for the X-ray diffraction studies

Compound	1	2
Empirical formula	$C_{34}H_{22}AuO_{11}PRu_3W$	$C_{39}H_{32}AuO_{11}PRu_3W$
M	1299.35	1391.68
Crystal system	Monoclinic	Orthorhombic
Space group	$P2_1/c$	$Pna2_1$
a/Å	9.031(2)	20.389(3)
b/Å	25.086(4)	16.226(3)
c/Å	16.238(3)	26.074(4)
β/°	95.75(2)	
U/Å^3	3660(1)	8626(2)
Crystal size/mm	0.18 × 0.20 × 0.22	0.20 × 0.30 × 0.45
Z	4	8
D_c/g cm^{-3}	2.358	2.143
F(000)	2447	5231
h, k, l ranges	−10 to 10, 0–29, 0–19	0–24, 0–19, 0–30
μ(Mo-Kα)/mm^{-1}	8.47	7.19
Transmission factors	1.00, 0.71	1.00, 0.61
No. of unique data	6434	7754
Data with $I > 2\sigma(I)$	4391	4556
No. of parameters	461	1009
R, R', S	0.036, 0.032, 1.14	0.040, 0.036, 1.75
Maximum Δ/σ ratio	0.003	0.041
Residual electron density/e Å^{-3}	0.90, −0.96	0.88, −0.89

* Features common to determinations: λ(Mo-Kα) = 0.709 30 Å, Nonius CAD-4 diffractometer, T 297 K, $R = \Sigma||F_o| - |F_c||/\Sigma|F_o|$, $R' = [\Sigma w(F_o - F_c)^2/\Sigma wF_o^2]^{\frac{1}{2}}$, $S = [\Sigma w|F_o - F_c|^2/(N_o - N_v)]^{\frac{1}{2}}$, $w^{-1} = \sigma^2(F)$ (N_o = number of observations; N_v = number of variables).

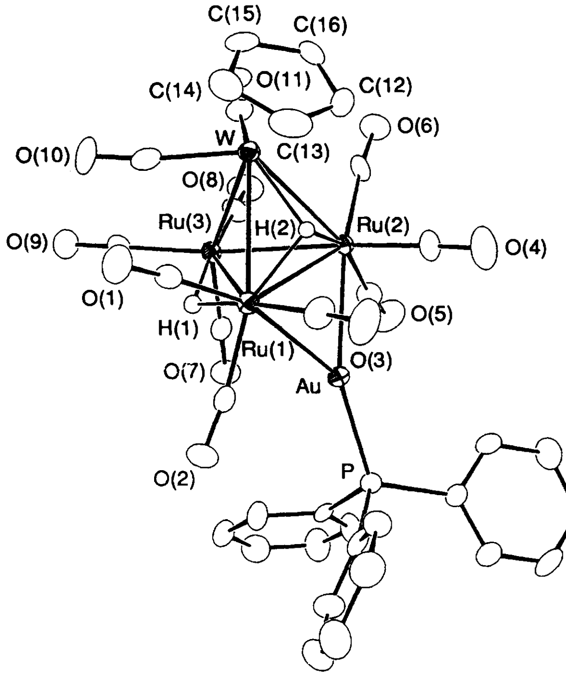

Fig. 1 Molecular structure of $[WRu_3(\eta\text{-}C_5H_5)(CO)_{11}(\mu\text{-}H)_2(AuPPh_3)]$ **1** showing the atomic numbering scheme

Spectral data of **1**: MS (FAB), m/z 1322 (M^+). IR (C_6H_{12}) ν(CO) 2090vw, 2063w, 2035vs, 2010vs, 1986s, 1949w (br) and 1879vw (br) cm^{-1}. NMR: ^{1}H (CD_2Cl_2, 210 K), δ 7.44–7.42 (m, 15 H, Ph), 5.31 (s, 5 H, C_5H_5), −8.26 [s, 1 H, J(W–H) 80.4 Hz] and −19.74 (s, 1 H); ^{31}P ($CDCl_3$, 297 K), δ 66.74 (s) (Found: C, 30.55; H, 1.70. $C_{34}H_{22}AuO_{11}PRu_3W$ requires C, 30.85; H, 1.65%).

Spectral data of **2**: MS (FAB), m/z 1392 (M^+). IR (C_6H_{12}) ν(CO) 2061s, 2019vs, 2004m(sh), 1991m, 1982m, 1953w(sh), 1940w (br) and 1871vw (br) cm^{-1}. NMR (CD_2Cl_2): ^{1}H (193 K), δ 7.59–7.55 (m, 15 H, Ph), 1.73 (s, C_5Me_5, **2a**), 1.70 (s, C_5Me_5, **2b**), −17.06 [s, **2b**, J(W–H) 51], −18.65 [s, **2b**, J(W–H) 49] and −19.07 [s, **2a**, J(W–H) 48 Hz]; ^{31}P (233 K), δ 69.29 (s, **2a**), 62.75 (s, **2b**) (Found: C, 33.50; H, 2.30. $C_{39}H_{32}AuO_{11}PRu_3W$ requires C, 33.65; H, 2.30%).

X-Ray Crystallography.—Diffraction measurements were carried out on a Nonius CAD-4 diffractometer. Lattice parameters of **1** were determined from 25 randomly selected high-angle reflections with 2θ angles in the range 19.20–28.10°, whereas the corresponding cell dimensions of complex **2** were determined from 25 reflections, with 2θ angles in the range 21.00–24.14°. All reflections were corrected for Lorentz, polarization and absorption effects. All data reduction and refinement were performed using the NRCC-SDP-VAX packages.[7] The structures were solved by direct methods and refined by full-matrix least squares; all non-hydrogen atoms were refined with anisotropic thermal parameters. For complex **1** the space group $P2_1/c$ was identified on the basis of systematic absences. The position of the bridging hydride ligand was obtained from a Fourier difference synthesis, included in the structure factor calculation and refined accordingly. Complex **2** crystallized in the orthorhombic system. Due to poor quality of the data, the hydrides were not located, but the hydrogen atoms on the organic ligands were placed in idealized positions and were included in the structure factor calculation. The combined data collection and refinement parameters are given in Table 1. Atomic positional parameters for complex **1** are given in Table 2, and selected bond distances and angles in Table 4. The corresponding parameters for **2** are given in Tables 3 and 5, respectively.

Additional material available from the Cambridge Crystallographic Data Centre comprises H-atom coordinates, thermal parameters and remaining bond lengths and angles.

Results and Discussion

Heterometal complexes $[WRu_3L(CO)_{12}(AuPPh_3)]$ (L = C_5H_5 or C_5Me_5) react with H_2 (1 atm) in refluxing thf solution to afford the hydride clusters $[WRu_3L(CO)_{11}(\mu\text{-}H)_2(AuPPh_3)]$ (L = C_5H_5 **1** or C_5Me_5 **2**) in near quantitative yield. The products can be easily purified by chromatography and recrystallization. The molecular structure of complex **1** was determined from a single-crystal X-ray diffraction study. The molecular geometry and the scheme used for labelling the atoms

Table 2 Atomic coordinates for complex **1**

Atom	x	y	z	Atom	x	y	z
Au	0.647 16(5)	0.909 331(19)	0.182 43(3)	C(22)	1.024 0(14)	0.970 4(6)	0.357 1(8)
W	0.401 44(5)	0.759 987(20)	0.031 68(3)	C(23)	0.849 6(13)	1.029 7(5)	0.212 4(7)
Ru(1)	0.404 34(10)	0.842 03(4)	0.166 01(5)	C(24)	0.920 7(16)	1.016 0(5)	0.143 0(8)
Ru(2)	0.647 00(10)	0.838 93(4)	0.054 91(5)	C(25)	1.010 7(17)	1.052 5(6)	0.108 5(8)
Ru(3)	0.634 16(10)	0.758 25(4)	0.171 25(5)	C(26)	1.027 3(14)	1.102 2(6)	0.141 8(8)
P	0.747 6(3)	0.978 60(13)	0.261 92(18)	C(27)	0.957 7(17)	1.115 9(5)	0.208 6(9)
C(1)	0.229 8(13)	0.803 9(5)	0.187 5(7)	C(28)	0.866 5(14)	1.080 4(5)	0.242 5(7)
C(2)	0.429 9(13)	0.876 4(5)	0.271 1(7)	C(29)	0.604 2(12)	1.014 2(4)	0.309 2(7)
C(3)	0.304 4(13)	0.901 2(5)	0.111 2(8)	C(30)	0.615 4(15)	1.029 8(5)	0.390 8(7)
C(4)	0.594 0(14)	0.898 7(5)	−0.015 2(7)	C(31)	0.500 7(17)	1.055 9(6)	0.422 6(8)
C(5)	0.842 7(13)	0.861 6(5)	0.094 2(7)	C(32)	0.369 6(15)	1.066 2(6)	0.374 5(9)
C(6)	0.718 5(14)	0.796 5(5)	−0.027 3(7)	C(33)	0.355 6(15)	1.050 9(6)	0.291 7(9)
C(7)	0.772 8(13)	0.791 4(5)	0.250 2(7)	C(34)	0.471 9(14)	1.025 2(5)	0.260 5(7)
C(8)	0.792 6(14)	0.726 1(6)	0.123 4(7)	O(1)	0.126 3(10)	0.782 9(4)	0.204 0(6)
C(9)	0.591 6(15)	0.699 2(5)	0.240 6(7)	O(2)	0.429 5(10)	0.893 0(4)	0.337 3(5)
C(10)	0.341 3(14)	0.707 9(5)	0.114 8(7)	O(3)	0.246 3(11)	0.937 6(4)	0.080 5(6)
C(11)	0.551 5(14)	0.706 0(5)	0.007 8(7)	O(4)	0.567 3(14)	0.935 0(4)	−0.054 6(6)
C(12)	0.302 6(14)	0.805 0(5)	−0.086 9(7)	O(5)	0.963 8(9)	0.873 4(4)	0.108 1(6)
C(13)	0.188 8(14)	0.802 1(6)	−0.034 6(8)	O(6)	0.773 0(11)	0.774 6(4)	−0.078 5(5)
C(14)	0.157 0(14)	0.748 3(6)	−0.023 4(8)	O(7)	0.857 3(10)	0.810 2(4)	0.298 5(5)
C(15)	0.253 4(16)	0.718 0(5)	−0.069 7(8)	O(8)	0.893 2(9)	0.704 9(4)	0.100 4(6)
C(16)	0.339 8(15)	0.753 4(6)	−0.108 0(6)	O(9)	0.574 8(12)	0.664 4(4)	0.281 7(5)
C(17)	0.876 1(12)	0.955 1(4)	0.347 4(7)	O(10)	0.289 3(11)	0.676 6(4)	0.153 7(6)
C(18)	0.829 0(14)	0.918 8(5)	0.403 1(7)	O(11)	0.618 9(10)	0.671 5(4)	−0.014 8(6)
C(19)	0.926 1(15)	0.897 9(5)	0.465 9(8)	H(1)	0.507(9)	0.795(4)	0.223(5)
C(20)	1.070 8(15)	0.914 9(6)	0.473 7(8)	H(2)	0.442(9)	0.883(3)	0.059(5)
C(21)	1.120 9(15)	0.950 0(6)	0.418 6(9)				

are shown in Fig. 1. Selected bond distances and angles are listed in Table 4. The tungsten atom and the three ruthenium atoms define a tetrahedral core structure, in which the gold atom of the $AuPPh_3$ fragment bridges a Ru–Ru bond and lies on the extension of a Ru_2W triangle, the tungsten atom is co-ordinated by a C_5H_5 ligand and two terminal CO ligands, and each of three basal ruthenium atoms is associated with three orthogonal terminal CO ligands. If it is assumed that the $AuPPh_3$ fragment acts as a one-electron donor to the Ru_3W core, this molecule has 60-valence electron count, consistent with that expected for tetrahedral cluster compounds.

The most interesting features of this molecule are the position and bonding mode of the hydride ligands which were located on the Fourier difference map. The X-ray analysis shows clearly that the edge-bridging hydride H(1) spans the Ru(1)–Ru(3) edge. This assignment is in agreement with the fact that this bond [2.949(1) Å] is longer than the Ru(2)–Ru(3) bond [2.779(1) Å] and that the angles Ru(3)–Ru(1)–C(1) [103.3(4)°] and Ru(1)–Ru(3)–C(9) [112.6(4)°] are much greater than the Ru–Ru–C angles of the corresponding Ru(1)–Ru(3) edge (86.9–96.4°) which has no interaction with bridging hydride. For the hydride atom H(2), a survey of interatomic angles within the molecule shows that the CO ligands on the W–Ru(1)–Ru(2) face are distorted away from the hydride ligand H(2). For instance that the W–Ru(1)–C(3) and W–Ru(2)–C(4) angles are 103.0(4) and 107.9(4)°, respectively, shows clearly that they are not perpendicular to the WRu_2 basal plane. However, the W–Ru(1)–C(1) [80.9(3)°] and W–Ru(2)–C(6) [80.6(4)°] angles for the CO ligands parallel to the Ru_2W plane show no such enlargement and are slightly smaller than the anticipated values (90°) for a pseudo-octahedral arrangement, due to the existence of a Ru–Au bond at the opposite position. Similar distortion of the CO ligands surrounding the face-bridging hydride was reported in the tetranuclear clusters $[Fe_3Pt(CO)_{10}(\mu_3\text{-}H)(\mu_3\text{-}COMe)(PPh_3)]$,[8] $[Co_3Fe(CO)_9(\mu_3\text{-}H)\{P(OMe)_3\}_3]$,[9] $[WOs_3(\eta\text{-}C_5H_5)(CO)_{10}(\mu_3\text{-}H)(C_2R_2)]$[10] (R = CO_2Et) and $[WRu_3(\eta\text{-}C_5Me_5)(CO)_{10}(\mu_3\text{-}H)(\mu_3\text{-}PPh)]$.[11] The solid-state bonding arrangements of the hydrides are somewhat inconsistent with the ^1H NMR spectrum in solution which shows two hydride signals at δ −8.26 [J(W–H) 80.4 Hz] and −19.74 at 180 K. The latter is clearly due to an edge-bridging Ru–H–Ru hydride but the signal at δ −8.26 is better identified as a terminal hydride because of its large J(W–H) coupling constant and the value of its chemical shift.[12] The transformation from a triply bridging to a terminal mode requires very little motion of hydrogen atom, therefore it is not violating the structural assignment in the solid state. No temperature dependent variation of the J(W–H) coupling (⩽2 Hz) was observed in the range 210–180 K. Above 210 K the hydride signals begin to broaden and collapse due to the rapid exchange of hydrides, so preventing the accurate measurement of the J(W–H) coupling constant.

The solution dynamics of **1** was also investigated by a variable-temperature ^{13}C NMR study. At 220 K, the spectrum gives one sharp W–CO resonance at δ 216.4 [J(W–C) 170 Hz] with relative intensity of 2 and five broad Ru–CO resonances at δ 208.3, 202.8, 196.9, 194.9 and 192.3 of relative intensities 2:2:2:1:2 (Fig. 2). This six-line pattern suggests that the molecule has a time-averaged mirror plane bisecting the W, H(2), Ru(3) and Au atoms and the midpoint of the Ru(2)–Ru(3) bond, which is generated by rapid and reversible hydride migration from one Ru–Ru edge to the second Ru–Ru edge (Scheme 2). The signal at δ 194.9 can be unambiguously assigned to the axial CO ligand on the unique Ru(3) atom because it lies on the plane of mirror symmetry. The hydride migration is frozen out at 190 K, causing the molecule to lose its C_s symmetry. Thus, all CO resonances, except the unique CO signal at δ 194.9, broaden and merge into the baseline. Conversely, elevation in temperature leads to exchange broadening and coalescence of all five Ru–CO resonances at about the same rate and a very broad signal is observed at δ 298.5 at 280 K. This behaviour is consistent with the interpretation that the Ru–CO ligands undergo rapid intermetallic CO exchange on the Ru_3 triangle or that the $AuPPh_3$ fragment rotates on the edges of the Ru_3 triangle along with the rapid hydride exchange. In general, many cluster complexes exhibit facile intermetallic CO exchange *via* pairwise terminal–bridge CO exchange[13] or in terms of the 'merry-go-round' type of movement.[14] Alternatively, migration of the $AuPPh_3$ should be considered on the basis of previous examples: the isobal

Table 3 Atomic coordinates for complex **2**

Atom	*x*	*y*	*z*	Atom	*x*	*y*	*z*
Au(1A)	0.982 68(6)	0.253 91(9)	0.173 80(4)	Au(1B)	0.261 15(6)	0.730 09(7)	0.077 42(5)
W(1A)	0.915 63(5)	0.252 89(8)	0.021 06(5)	W(1B)	0.329 98(6)	0.739 45(8)	0.231 73(5)
Ru(1A)	1.026 90(11)	0.326 46(14)	0.087 38(10)	Ru(1B)	0.218 22(12)	0.808 23(15)	0.165 57(10)
Ru(2A)	1.002 25(11)	0.148 43(14)	0.094 05(10)	Ru(2B)	0.244 08(12)	0.630 47(14)	0.163 10(10)
Ru(3A)	1.053 12(12)	0.221 24(15)	0.004 84(10)	Ru(3B)	0.192 87(12)	0.708 37(17)	0.250 30(10)
P(1A)	0.951 1(4)	0.261 8(6)	0.259 4(3)	P(1B)	0.291 2(4)	0.739 1(5)	−0.006 2(3)
C(1A)	0.916 9(16)	0.157 0(24)	−0.026 6(12)	C(1B)	0.325 2(14)	0.655 6(21)	0.287 7(14)
C(2A)	0.955 0(16)	0.323(3)	−0.032 2(12)	C(2B)	0.293 3(16)	0.808 6(22)	0.288 6(13)
C(3A)	1.048 4(17)	0.418 6(25)	0.038 9(16)	C(3B)	0.191 4(19)	0.901 1(22)	0.201 1(13)
C(4A)	1.109 4(16)	0.323(3)	0.116 5(16)	C(4B)	0.139 7(16)	0.794 3(24)	0.137 7(14)
C(5A)	0.999 7(15)	0.407 6(18)	0.140 8(10)	C(5B)	0.243 6(20)	0.887 6(22)	0.111 2(13)
C(6A)	1.081 6(15)	0.119 8(17)	0.125 9(12)	C(6B)	0.167 7(17)	0.596 9(24)	0.134 4(15)
C(7A)	0.950 9(15)	0.094 5(17)	0.146 0(12)	C(7B)	0.294 4(14)	0.573 4(19)	0.112 3(13)
C(8A)	1.003 7(17)	0.055 4(18)	0.049 9(11)	C(8B)	0.242 3(23)	0.540(3)	0.206 7(16)
C(9A)	1.056 3(15)	0.139 6(20)	−0.046 1(11)	C(9B)	0.194 8(17)	0.628 0(21)	0.304 7(12)
C(10A)	1.090 7(13)	0.305 4(18)	−0.037 4(12)	C(10B)	0.154 0(15)	0.789 9(20)	0.293 8(13)
C(11A)	1.136 1(12)	0.186 9(21)	0.029 0(12)	C(11B)	0.114 8(18)	0.667(3)	0.223 8(14)
C(12A)	0.862 7(13)	0.275 7(18)	0.259 8(11)	C(12B)	0.379 7(12)	0.759 2(16)	−0.014 4(9)
C(13A)	0.821 6(16)	0.202 8(19)	0.266 8(15)	C(13B)	0.422 6(14)	0.691 4(21)	−0.011 7(13)
C(14A)	0.753 2(14)	0.208 5(23)	0.268 1(13)	C(14B)	0.485 7(20)	0.693(3)	−0.005 9(17)
C(15A)	0.734 9(15)	0.292 8(21)	0.254 6(12)	C(15B)	0.511 7(16)	0.787(3)	−0.010 1(15)
C(16A)	0.766 7(17)	0.357 4(22)	0.251 6(17)	C(16B)	0.466 3(21)	0.853 3(24)	−0.012 6(18)
C(17A)	0.833 4(16)	0.350 9(19)	0.254 1(14)	C(17B)	0.405 2(15)	0.833 9(19)	−0.016 3(15)
C(18A)	0.981 4(13)	0.172 3(19)	0.298 9(12)	C(18B)	0.272 0(14)	0.648 8(15)	−0.042 8(10)
C(19A)	0.960 8(14)	0.153 5(18)	0.348 4(13)	C(19B)	0.303 2(16)	0.626 1(22)	−0.085 2(12)
C(20A)	0.985 8(17)	0.089 1(22)	0.373 6(13)	C(20B)	0.283 0(17)	0.559 6(22)	−0.117 5(17)
C(21A)	1.035 8(16)	0.044 4(19)	0.351 6(14)	C(21B)	0.231 3(19)	0.518 8(21)	−0.101 1(15)
C(22A)	1.054 8(16)	0.055 2(21)	0.309 3(14)	C(22B)	0.195 4(17)	0.538 3(22)	−0.054 2(15)
C(23A)	1.027 9(14)	0.118 7(20)	0.280 2(11)	C(23B)	0.215 6(15)	0.603 4(19)	−0.028 5(12)
C(24A)	0.985 4(17)	0.349 9(20)	0.297 7(12)	C(24B)	0.251 0(14)	0.827 9(17)	−0.040 2(9)
C(25A)	0.953 5(17)	0.390 3(23)	0.340 1(15)	C(25B)	0.272 6(19)	0.859 0(22)	−0.087 8(13)
C(26A)	0.988 8(24)	0.447 4(24)	0.362 9(14)	C(26B)	0.241 7(17)	0.921 5(20)	−0.113 2(13)
C(27A)	1.048 6(18)	0.475 0(18)	0.345 4(13)	C(27B)	0.192 8(20)	0.951 2(24)	−0.090 5(14)
C(28A)	1.077 7(20)	0.447 4(21)	0.309 0(15)	C(28B)	0.168 6(20)	0.936 5(24)	−0.042 2(15)
C(29A)	1.048 2(16)	0.382 7(22)	0.283 4(14)	C(29B)	0.201 1(14)	0.868 4(18)	−0.017 1(10)
C(30A)	0.809 4(13)	0.208 2(18)	0.023 1(12)	C(30B)	0.437 8(13)	0.696 4(19)	0.237 3(13)
C(31A)	0.815 0(11)	0.276 5(18)	−0.013 3(11)	C(31B)	0.428 0(12)	0.769 4(21)	0.268 0(10)
C(32A)	0.831 5(13)	0.350 6(17)	0.011 5(11)	C(32B)	0.410 7(14)	0.834 9(17)	0.237 4(11)
C(33A)	0.834 8(13)	0.332 7(19)	0.063 5(13)	C(33B)	0.413 9(14)	0.803 8(18)	0.183 9(11)
C(34A)	0.823 8(14)	0.247 2(24)	0.070 2(10)	C(34B)	0.430 3(11)	0.723 5(17)	0.184 3(10)
C(35A)	0.781 3(15)	0.125 8(20)	0.013 3(14)	C(35B)	0.464 8(17)	0.614 2(24)	0.256 5(17)
C(36A)	0.799 7(14)	0.270 9(23)	−0.069 0(10)	C(36B)	0.446 2(17)	0.777(3)	0.320 2(15)
C(37A)	0.834 9(19)	0.434 3(21)	−0.008 0(16)	C(37B)	0.406 8(16)	0.928 6(18)	0.251 6(13)
C(38A)	0.836 9(18)	0.393(3)	0.108 0(14)	C(38B)	0.408 6(21)	0.868(3)	0.138 4(16)
C(39A)	0.811 0(14)	0.205 3(22)	0.124 2(11)	C(39B)	0.439 0(15)	0.656 5(24)	0.142 7(15)
O(1A)	0.910 5(13)	0.100 4(16)	−0.052 5(10)	O(1B)	0.333 6(12)	0.601 5(18)	0.317 1(11)
O(2A)	0.960 3(12)	0.354 5(15)	−0.073 6(8)	O(2B)	0.282 3(12)	0.852 9(17)	0.320 7(9)
O(3A)	1.064 1(15)	0.469 5(14)	0.015 2(11)	O(3B)	0.173 9(16)	0.953 7(15)	0.231 0(13)
O(4A)	1.160 8(13)	0.312 9(22)	0.134 8(12)	O(4B)	0.089 7(12)	0.782 3(22)	0.118 8(12)
O(5A)	0.992 7(12)	0.460 7(13)	0.164 2(9)	O(5B)	0.259 2(16)	0.940 3(15)	0.086 9(10)
O(6A)	1.129 3(11)	0.102 8(17)	0.150 3(11)	O(6B)	0.120 0(13)	0.573 8(18)	0.111 8(12)
O(7A)	0.918 9(11)	0.055 6(13)	0.174 6(8)	O(7B)	0.328 0(13)	0.537 0(13)	0.084 9(10)
O(8A)	1.007 0(15)	−0.005 4(13)	0.029 1(10)	O(8B)	0.245 4(18)	0.483 1(15)	0.233 4(11)
O(9A)	1.059 4(11)	0.093 2(15)	−0.080 6(10)	O(9B)	0.188 8(12)	0.578 0(15)	0.333 7(9)
O(10A)	1.117 6(13)	0.350 2(19)	−0.065 2(10)	O(10B)	0.128 1(10)	0.837 0(14)	0.319 8(9)
O(11A)	1.185 6(10)	0.162 9(18)	0.043 8(10)	O(11B)	0.061 3(12)	0.645 1(25)	0.212 8(12)

HgY^+ fragments [Y = halide, CF_3 or Mo (η-C_5H_5)$(CO)_3$] are highly mobile on the surface of an Os_{10} cluster core,[15] a μ-$AuPPh_3$ fragment undergoes phosphine-promoted decapping to give an anionic cluster and $Au(PPh_3)_2{}^+$ in solution,[16] and the $(AuPPh_3)_2$ fragment participates in a process called partial Berry pseudo-rotation which leads to the exchange of Au atom environments over the face of a Ru_3 triangle.[17] We cannot rule out either process on the basis of our experimental data. However, the W–CO signal begins to collapse at 180 K, suggesting the facile exchange of W–CO and the CO ligands on the Ru atoms. This observation can be explained by intermetallic CO exchange.

The derivative **2** was examined by single-crystal X-ray analysis, since the NMR data (see below) suggested that this compound adopts a completely different geometry in solution to that of **1**. The molecule crystallizes in the orthorhombic system and the asymmetric unit contains two crystallographically distinct, but structurally similar molecules. A view of one of the molecules is shown in Fig. 3; selected bond distances and angles for molecule A are given in Table 5. Complex **2** is structurally related to the previously reported trihydride complex **3**,[18] and can thus be regarded as a derivative generated by replacing the unique Ru–H–Ru hydride with the Au atom from the isolobal $AuPPh_3$ fragment. The core geometry can be described as a planar triangulated $AuRu_3$ core [dihedral angle between the Ru_3 and $AuRu_2$ triangles 175.5(1)° and between the Ru_2W and $AuRu_2$ triangles 114.3(1)°] with the Ru_3 triangle capped by a W atom. This feature is in contrast to that observed

Table 4 Selected bond lengths (Å) and angles (°) for complex **1** with estimated standard deviations (e.s.d.s) in parentheses

Au-Ru(1)	2.759(1)	Au-Ru(2)	2.722(1)
W-Ru(1)	2.997(1)	W-Ru(2)	2.969(1)
W-Ru(3)	2.933(1)	Ru-Ru(2)	2.976(1)
Ru(1)-Ru(3)	2.949(1)	Ru(2)-Ru(3)	2.779(1)
Au-P	2.296(3)	Ru(1)-H(1)	1.72(9)
Ru(1)-H(2)	1.82(8)	Ru(2)-H(2)	1.87(8)
Ru(3)-H(1)	1.74(8)	W-H(2)	1.90(8)
W-CO(mean)	1.98(1)	Ru-CO(mean)	1.90(1)
W-Ru(1)-C(3)	103.0(4)	W-Ru(2)-C(4)	107.9(4)
W-Ru(1)-C(1)	80.9(3)	W-Ru(2)-C(6)	80.6(4)
Ru(3)-Ru(1)-C(1)	103.3(4)	Ru(3)-Ru(1)-C(2)	105.9(4)
Ru(1)-Ru(3)-C(7)	97.0(3)	Ru(1)-Ru(3)-C(9)	112.6(4)
Ru(2)-Ru(3)-C(7)	94.0(3)	Ru(2)-Ru(3)-C(8)	86.9(4)
Ru(3)-Ru(2)-C(5)	95.2(4)	Ru(3)-Ru(2)-C(6)	96.4(4)
W-CO(mean)	169(1)	Ru-CO(mean)	175(1)

Table 5 Selected bond lengths (Å) and angles (°) for molecule A of complex **2** with e.s.d.s in parentheses

Au(1)-Ru(1)	2.697(3)	Au(1)-Ru(2)	2.723(3)
W(1)-Ru(1)	3.092(3)	W(1)-Ru(2)	3.101(3)
W(1)-Ru(3)	2.880(3)	Ru(1)-Ru(2)	2.937(3)
Ru(1)-Ru(3)	2.799(3)	Ru(2)-Ru(3)	2.807(4)
Au(1)-P(1)	2.326(8)		
W-CO(mean)	1.98(4)	Ru-CO(mean)	1.92(3)
W(1)-Ru(1)-C(3)	96(1)	W(1)-Ru(1)-C(5)	116(1)
W(1)-Ru(2)-C(7)	112(1)	W(1)-Ru(2)-C(8)	94(1)
W(1)-Ru(3)-C(9)	105(1)	W(1)-Ru(3)-C(10)	110(1)
W-CO(mean)	164(3)	Ru-CO(mean)	173(3)

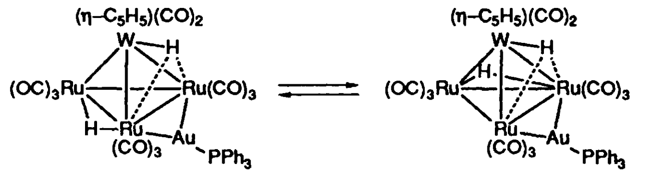

Scheme 2

for **1**, in which the $AuPPh_3$ takes up the extension of the Ru_2W triangle [dihedral angle between the Ru(1), Ru(2), Ru(3) and Au, Ru(1), Ru(2) triangles 106.14(3)° and between the W, Ru(1), Ru(2) and Au, Ru(1), Ru(2) triangles 177.35(3)°], and can be viewed as a triangulated $AuRu_2W$ core arrangement with a $Ru(CO)_3$ fragment bridged on the Ru_2W triangle. The hydride ligands have not been located in this case, but it is obvious that both hydrides are associated with the W(1)-Ru(1) and W(1)-Ru(2) edges because of the elongation of these W-Ru bonds (3.092, 3.101 Å) with respect to the third W-Ru bond [2.880(3) Å] and the Ru-Ru bonds (2.799-2.937 Å) in the molecule. The arrangement of the hydride and the $AuPPh_3$ ligands is reminiscent of the related tetrahedral $NiOs_3$ complexes $[NiOs_3(\eta\text{-}C_5H_5)(CO)_9(\mu\text{-}H)_2(AuPPh_3)]$ [19] and $[NiOs_3(\eta\text{-}C_5H_5)(CO)_9(\mu\text{-}H)_2(CuPPh_3)]$,[20] in which the hydrides are associated with two Os-Os edges and the $MPPh_3$ fragment spans the third Os-Os edge, forming a planar triangulated $NiOs_2M$ arrangement.

The solution properties of the C_5Me_5 derivative were explored by NMR spectroscopy, and were found to be more complicated than for the C_5H_5 derivative. The ^{31}P NMR spectrum at room temperature exhibits a broad signal at δ 68.1 and we observed two sharp signals at δ 69.29 and 62.75 in a ratio 9:1 upon decreasing the temperature to 233 K. This observation strongly indicates the coexistence of two tautomers which undergo rapid equilibration in solution. Similarly, the ^1H NMR spectrum gives a very broad hydride signal at 297 K and

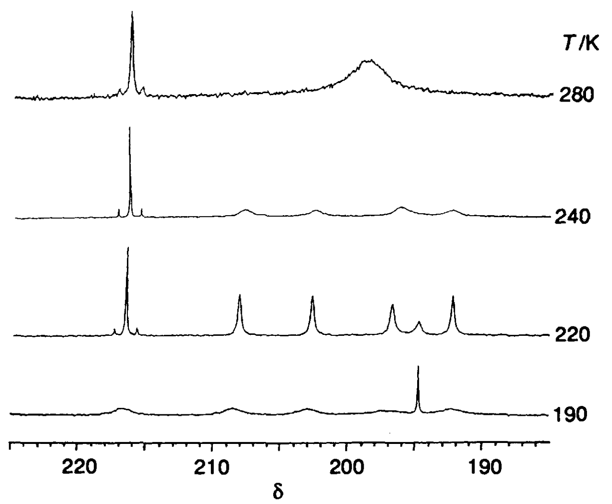

Fig. 2 Variable-temperature ^{13}C NMR spectra (400 MHz, CD_2Cl_2) of complex **1**, showing the region of CO resonances

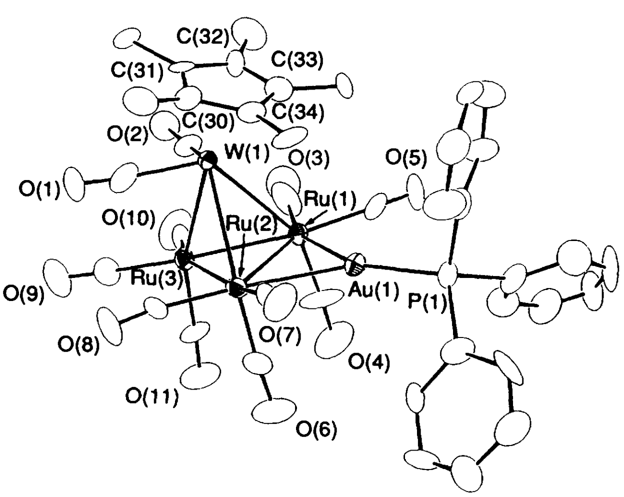

Fig. 3 Perspective drawing of $[WRu_3(\eta\text{-}C_5Me_5)(CO)_{11}(\mu\text{-}H)_2(AuPPh_3)]$ **2** with numbering of atoms. This compound crystallizes with two independent molecules in the unit cell; only the structure of molecule A is shown

on lowering the temperature to 193 K we observed the formation of three hydride signals at δ −17.06 [J(W-H) 51], −18.65 J(W-H) 49] and −19.07 [J(W-H) 48 Hz] in an intensity ratio 1:1:18, respectively. The hydride signal at δ −19.07 is clearly due to the tautomer **2a** which adopts the structure found in the solid state with two equivalent W-H-Ru ligands. Because of the observation of J(W-H) coupling, the hydride signals at δ −17.06 and −18.65 are assigned to an isomer **2b**, in which the hydride ligands occupy two inequivalent W-H-Ru sites (Scheme 3).

The variable-temperature ^{13}C NMR spectra were also recorded in order to probe the dynamic motion of CO ligands. The spectrum at 193 K exhibits six intense signals at δ 225.0 [J(W-C) 153], 212.8 [J(P-C) 8 Hz], 205.5, 200.6 [J(P-C) 13 Hz], 199.9 and 196.1, with ratio 2:2:1:2:2:2, due to the major tautomer **2a**; the peaks of the minor isomer **2b** were not observed under these conditions. From the J(P-C) coupling constants and the exchange behaviour due to the localized tripodal rotation observed for the $Ru(CO)_3$ signals at δ 205.5 and 199.9, we can unambiguously assign the peaks at δ 200.6, 205.5 and 199.9 to the CO ligands *trans* to the $AuPPh_3$ fragment, the axial and two equatorial CO on the unique Ru atom, respectively. Finally, the rapid tautomerization of **2a** and **2b** and, possibly, the intermetallic hydride together with

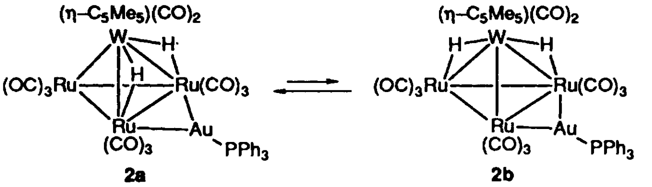

Scheme 3

$AuPPh_3$ migration causes the collapse of all CO signals on warming to 263 K.

Conclusion

The cyclopentadienyl derivative **1** exhibits a tetrahedral core in which one hydride ligand caps a Ru_2W triangle and the second bridges a Ru–Ru edge and undergoes rapid migration to the second Ru–Ru edge at low temperature. However, for complex **2**, both hydrides are associated with the W–Ru edges, which are related by a plane of symmetry in the solid state, and undergo migration to form two rapidly interconverting isomers in solution. The minor component **2b** possesses a cluster core similar to **2a**; however, the hydride ligands occupy two non-equivalent W–H–Ru sites. This alignment of the hydride and $AuPPh_3$ ligand is different from that of the zigzag sequence of hydrides in $[Mo(\eta\text{-}C_5H_5)Ru_3(CO)_{11}(\mu\text{-}H)_3]$[3a] and in the minor isomer of complexes **3** and **5**.[2b] Apparently, the electron-donating ability of the C_5Me_5 ligand[21] has caused a build-up of negative charge on the W atom and this charge attracts the electropositive, bridging hydrides to the W–Ru edges.

Acknowledgements

We thank the National Science Council of the Republic of China (Grant No. NSC 82-0208-M007-079) and National Tsing Hua University for financial support.

References

1 D. A. Roberts and G. L. Geoffroy, in *Comprehensive Organometallic Chemistry*, eds. G. Wilkinson, F. G. A. Stone and E. W. Abel, Pergamon, Oxford, 1982, vol. 6, ch. 40; R. D. Adams, in *The Chemistry of Metal Clusters*, eds. D. F. Shriver, H. D. Kaesz and R. D. Adams, VCH, New York, 1990, ch. 3.
2 (*a*) Y. Chi, F.-J. Wu, B.-J. Liu, C.-C. Wang and S.-L. Wang, *J. Chem. Soc., Chem. Commun.*, 1989, 873; (*b*) Y. Chi, C.-Y. Cheng and S.-L. Wang, *J. Organomet. Chem.*, 1989, **378**, 45.
3 (*a*) C. E. Housecroft, D. M. Matthews, A. L. Rheingold and X. Song, *J. Chem. Soc., Dalton Trans.*, 1992, 2855; (*b*) L.-H. Hsu, W.-L. Hsu, D.-Y. Jan and S. G. Shore, *Organometallics*, 1986, **5**, 1041.
4 J. W. Koepke, J. R. Johnson, S. A. R. Knox and H. D. Kaesz, *J. Am. Chem. Soc.*, 1975, **97**, 3947.
5 M. Cazanoue, N. Lugan, J.-J. Bonnet and R. Mathieu, *Organometallics*, 1988, **7**, 2480.
6 B. F. G. Johnson, R. Khattar, J. Lewis and P. R. Raithby, *J. Chem. Soc., Dalton Trans.*, 1989, 1421.
7 E. J. Gabe, Y. LePage, J. P. Charland, F. L. Lee and P. S. White, *J. Appl. Crystallogr.*, 1989, **22**, 384.
8 M. Green, K. A. Mead, R. Mills, I. D. Salter, F. G. A. Stone and P. Woodward, *J. Chem. Soc., Chem. Commun.*, 1982, 51.
9 B. T. Huie, C. B. Knobler and H. D. Kaesz, *J. Am. Chem. Soc.*, 1978, **100**, 3059.
10 J. T. Park, J. R. Shapley, C. Bueno, J. W. Ziller and M. R. Churchill, *Organometallics*, 1988, **7**, 2307.
11 R.-C. Lin, Y. Chi, S.-M. Peng and G.-H. Lee, *Inorg. Chem.*, 1992, **31**, 3818.
12 A. P. Humphries and H. D. Kaesz, *Prog. Inorg. Chem.*, 1979, **25**, 146.
13 J. Washington and J. Takats, *Organometallics*, 1990, **9**, 928.
14 A. Riesen, F. W. B. Einstein, A. K. Ma, R. K. Pomeroy and J. A. Shipley, *Organometallics*, 1991, **10**, 3629.
15 L. H. Gade, B. F. G. Johnson and J. Lewis, *J. Chem. Soc., Dalton Trans.*, 1992, 933.
16 J. Evans, A. C. Street and M. Webster, *Organometallics*, 1987, **6**, 794.
17 C. J. Brown, P. J. McCarthy and I. D. Salter, *J. Chem. Soc., Dalton Trans.*, 1990, 3583; A. G. Orpen and I. D. Salter, *Organometallics*, 1991, **10**, 111.
18 M. R. Churchill, F. J. Hollander, J. R. Shapley and D. S. Foose, *J. Chem. Soc., Chem. Commun.*, 1978, 534; M. R. Churchill and F. J. Hollander, *Inorg. Chem.*, 1979, **18**, 161.
19 P. Braunstein, J. Rosé, A. M. Manotti-Lanfredi and A. Tiripicchio, *J. Chem. Soc., Dalton Trans.*, 1984, 1843.
20 F. Castagno, M. Castiglioni, E. Sappa, A. Tiripicchio, M. Tiripicchio Camellini, P. Braunstein and J. Rosé, *J. Chem. Soc., Dalton Trans.*, 1989, 1477.
21 (*a*) F. G. Bordwell and M. J. Bausch, *J. Am. Chem. Soc.*, 1983, **105**, 6188; (*b*) E. J. Miller, S. J. Landon and T. B. Brill, *Organometallics*, 1985, **4**, 533.

Received 5th January 1993; *Paper* 3/00061C